

# Diphoton production from quark–gluon plasma and hadronic matter

K.L. Haglin<sup>a</sup>

Department of Physics and Astronomy, St. Cloud State University, 720 Fourth Avenue South, St. Cloud, MN 56301, USA

Received: 9 August 2006 /

Published online: 8 November 2006 – © Springer-Verlag / Società Italiana di Fisica 2006

**Abstract.** The rate of diphoton production is calculated from a quark–gluon plasma and compared with the rate from hadronic matter. Background diphotons are identified and quantified, including effects from hadronic form factors. Robust thermometry and spectroscopy are shown to be possible owing to the structure of the expected invariant mass spectrum. Charmonium could also be probed with diphotons.

**PACS.** 25.75.-q; 13.85.Qk

## 1 Introduction

The formalism and technology for utilizing electromagnetic probes as a means of studying strongly interacting matter is well developed and documented [1, 2]. Further developments are indeed likely as experimental results become available at the relativistic heavy-ion collider (RHIC) and as interpretations are proposed and tested [3]. Mean free paths for particles interacting solely electromagnetically are many times greater than system sizes relevant for high-energy nuclear reactions. These electromagnetic signals will therefore carry undisturbed information to the detectors. Photon production offers essentially thermometry and mean kinematics to be probed, while dileptons offer spectroscopy and collective effects to be brought out for study [4]. Dileptons are more rarely produced than real photons since the production rate is one power of  $\alpha$  higher. Still, their kinematic structures make them attractive, if not desirable. Diphotons are the same order as dileptons in the fine structure constant, namely of the order  $\alpha^2$  and are therefore equally rare. While their production rate is small, it is not vanishingly small. They too carry information on their production mechanisms since different mechanisms will have rather different mass dependences. Finally, they are robust in the sense that their mass spectrum is insensitive to effects of flow.

Electromagnetic radiation persists during the entire evolution of the heated and compressed nuclear matter. Emission from quark matter must be quantified for early stages of the nuclear reactions and hadronic matter must be considered for late stages of the fireball. A compari-

son of the rates would make a useful beginning exploratory study.

## 2 Quark–antiquark annihilation

The rate for diphoton production is proportional to the photon self-energy, which is related to the full and bare propagators. At the two-loop level the self-energy comprises a quark loop with a photon internal line. Using cutting rules results in a pair of graphs describing the physical annihilation process  $q\bar{q} \rightarrow \gamma\gamma$  exhibiting  $t$  and  $u$  channel processes with an intermediate quark in each case. For massless quarks the amplitude is singular and requires regularization. Resummation techniques within finite-temperature field theory introduce screening effects to render the rate finite [5]. As a function of diphoton mass  $M$  it can be written as [6]

$$\frac{dR}{dM^2} = \frac{\sum_q e_q^4 \alpha^2}{4\pi^3} N_c \left[ \frac{\pi M T^3}{2} \right]^{1/2} e^{-M/T} \ln \left( \frac{cM^2}{\alpha_s T^2} \right), \quad (1)$$

where the constant  $c \simeq 0.042$  when a thermal fermion mass is taken to be  $m_f^2 = (2\pi/3)\alpha_s T^2$ . The expression is reliable for  $M > T$ , at high values of temperature.

Roughly speaking, the thermal behavior is manifest in the exponential function of the quantity mass over temperature; screening effects are responsible for the logarithmic dependence on mass, and finally, phase space and relative velocity effects are prevalent in the prefactor of the square root of the mass. The pieces themselves are therefore reasonably intuitive even though the details leading up to (1) are lengthy and not too transparent.

<sup>a</sup> e-mail: klhaglin@stcloudstate.edu

### 3 Hadron processes

The lowest-order (background) processes to consider in the hadron sector are annihilation processes  $h\bar{h} \rightarrow \gamma\gamma$  (where  $h$  is one of the low-lying mesons  $\pi$ ,  $K$ ,  $\rho$ ,  $\omega$ ,  $\phi$ ,  $a_1$ , ...). The rate for photon pair production is again proportional to the self-energy. A diagrammatic expansion picks off the lowest-order amplitudes and then requires a model for describing the interactions among the hadrons. Here a chiral Lagrangian is used [7]

$$\mathcal{L} = \frac{F_\pi^2}{8} \text{Tr} D_\mu U D^\mu U^\dagger, \quad (2)$$

where  $U = \exp(2i\phi/F_\pi)$ ,  $\phi$  is the multiplet of pseudoscalar mesons, and the covariant derivative  $D_\mu U = \partial_\mu U - igA_\mu^L U + igUA_\mu^R$  introduces vector and axial vector mesons. Specific gauging procedures are taken to ensure a description of pseudoscalar and vector mesons carrying the symmetry through to the interactions. This symmetry is then used to identify the structure of the multitude of interactions possible, but then the coupling constants in each case are adjusted to match the leading experimental hadronic decay rates.

Given the set of hadronic interactions embedded in the chiral Lagrangian, a description is available for the scattering amplitudes for various processes such as  $\pi^+\pi^- \rightarrow \gamma\gamma$ ,  $K^+K^- \rightarrow \gamma\gamma$ ,  $\rho^+\rho^- \rightarrow \gamma\gamma$ , and others. However, there are processes that are outside the scope of the chiral Lagrangian. In particular, processes that require a description of vertices of the types  $AVP$  and  $VVP$ , where  $A$  signifies an axial vector,  $V$  represents a vector meson, and  $P$  is a pseudoscalar meson. These are taken to be

$$\mathcal{L}_{VVP} = \tilde{g}\epsilon_{\mu\nu\alpha\beta}\partial^\mu V^\nu\partial^\alpha V^\beta, \quad (3)$$

following Wess–Zumino-type interactions and

$$\mathcal{L}_{AVP} = g'A_\mu V^{\mu\nu}\partial_\nu P. \quad (4)$$

Again, the coupling strength in each case is adjusted to match the empirical hadronic decays. Vector meson dominance is then used to identify the lowest-order radiative decay vertices. The above interactions are clearly not unique but simply represent a reasonable choice to assess the overall strength of each process. It is known, for example, that the choice of the  $AVP$  Lagrangian taken here cannot describe simultaneously all of the decay features known for  $a_1 \rightarrow \pi\rho$ . Since the purpose here is merely to do an inventory of hadronic processes and identify their relative importances, these choices are sufficient.

#### 3.1 Hadron–hadron annihilation

Keeping with the methods suggested above, a diagrammatic (lowest-order) approximation to the hadronic rate for producing pairs of photons from  $h\bar{h} \rightarrow \gamma\gamma$  can be written as

$$\frac{dR}{dM^2} = \frac{\mathcal{N}}{32\pi^4} \left(\frac{T}{M}\right) \lambda(M^2, m_h^2, m_h^2) \sigma(M) \times K_1(M/T), \quad (5)$$

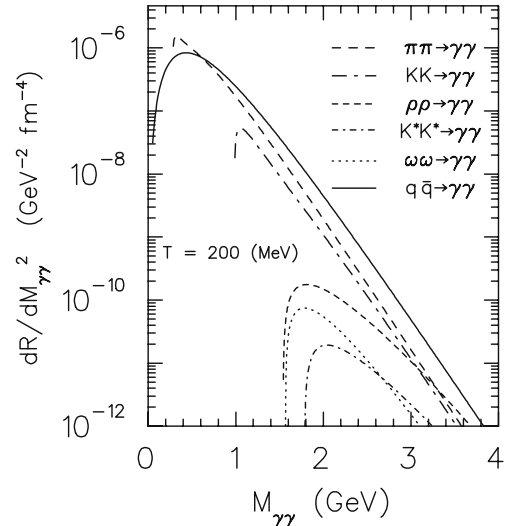


**Fig. 1.** Thermal rate for diphoton production from quark–antiquark annihilation as compared with leading hadron–hadron annihilation

where  $\mathcal{N}$  is a degeneracy to count the states,  $\lambda$  is the kinematic function describing two-body phase space,  $\sigma(M)$  is the cross section for  $h\bar{h} \rightarrow \gamma\gamma$ , and  $K_1$  is a modified Bessel function typical of these types of thermal rates. Details for the cross sections are not presented here due to space limitations but given the set of hadronic interactions and the coupling constants, a straightforward, albeit lengthy task ensues to produce the cross sections.

Having the annihilation cross sections, the rates are therefore readily calculable. The most important channels are shown in Fig. 1 and compared with the quark rate from (1). A fixed temperature of  $T = 200$  MeV is chosen to facilitate comparison with earlier estimates. A more appropriate comparison might take place at  $T_c = 170$  MeV. And yet, the relative comparison is robust to relatively small changes in temperature. The notable features are the common mass dependence, the very similar overall magnitudes of all the rates, and the threshold effects. An inevitable conclusion from the graph is that hadronic matter and quark matter produce photon pairs nearly equally at this temperature.

At higher invariant mass there are processes of the types  $\phi\phi \rightarrow \gamma\gamma$ ,  $a_1^+a_1^- \rightarrow \gamma\gamma$ ,  $b_1^+b_1^- \rightarrow \gamma\gamma$ , and several others that could become relevant.

#### 3.2 Meson decay into diphotons

The list of mesons decaying thermally in a heavy-ion context and able to produce photon pairs is fairly long. Mesons with significant branching to diphotons are  $\sigma$ ,  $f_2(1270)$ ,  $f_1(1285)$ ,  $a_2(1320)$ ,  $f_2'(1525)$ , and others. As well, in the charm sector there are  $\eta_c(2980)$ ,  $\chi_{c0}$ , and  $\chi_{c2}$  states with sizable branchings to two photons. The thermal rate for decay is an integral over available phase space of the vacuum decay rate weighted by thermal occupation convolved with a Breit–Wigner spectral density of the parent particle’s

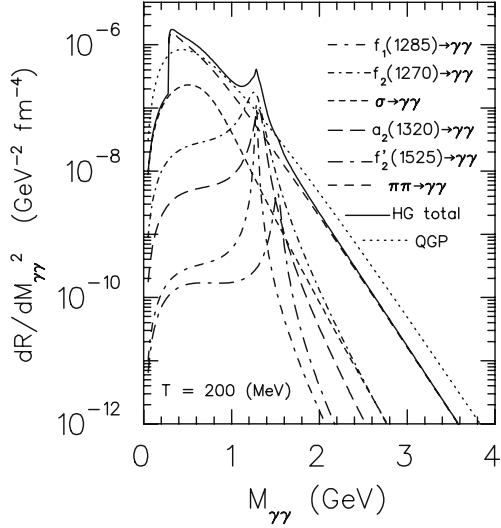


**Fig. 2.** Thermal meson decay rates into diphotons as well as the total hadron rate (*solid line*) compared again to the quark–antiquark annihilation rate

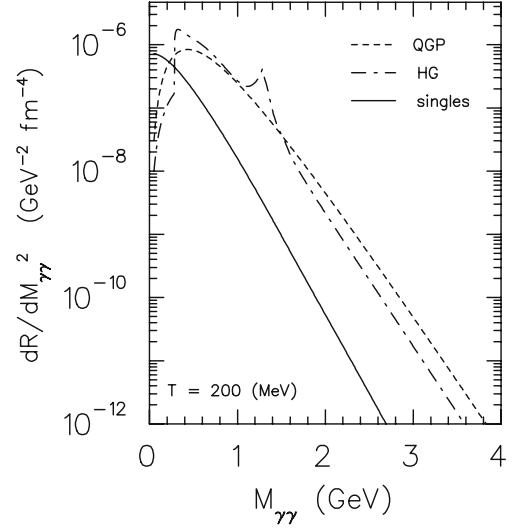


**Fig. 3.** Singles contributing to diphoton mass spectrum as compared with the total rates from hadronic matter and quark matter

mass. The expression can be simplified to the following form:

$$\frac{dR}{dM^2} = \frac{\mathcal{N}_a 4M^3}{(2\pi)^3} \Gamma(a \rightarrow \gamma\gamma) \times \frac{M\Gamma}{(M^2 - m_a^2)^2 + (M\Gamma)^2} \sum_{s=1}^{\infty} \frac{K_1(sM/T)}{(sM/T)}. \quad (6)$$

The degeneracy  $\mathcal{N}_a$  includes spin alone since neutral parents alone can decay into photon pairs. Also, the sum over integers  $s$  comes about owing to the choice of Bose–Einstein distributions (instead of Boltzmann) to more accurately reflect the quantum nature of the degrees of freedom.

The rates for leading decays are displayed in Fig. 2 along with the quark–antiquark annihilation rate. Meson decays are added to the hadron–hadron annihilation rates in order to arrive at a total hadron rate for a convenient comparison to the quark rate. The structure present is potentially very important to note. Decays of  $f_2(1270)$  and  $f_1(1285)$  are somewhat reminiscent of  $\rho$  and  $\omega$  decays into dileptons in the sense that there are two overlapping resonances, one rather narrow and one broad. They protrude above the background in a mass spectrum and therefore suggest spectroscopy studies, especially in the context of searching for possible medium effects.

#### 4 Singles masquerading as doubles

The rate for producing single photons is known to lowest order in the fine structure constant to be proportional to  $\alpha$ . Therefore the rate for producing uncorrelated doubles from two (unrelated) processes is of the order  $\alpha^2$ . It is therefore possible that the diphoton rate could be masked behind two singles having kinematics such that their mass

is the same as the diphoton under consideration. The rate for producing two photons with invariant mass  $M$  is

$$\frac{dR}{dM^2} = \left( E_1 \frac{dR}{d^3p_1} \right) \left( E_2 \frac{dR}{d^3p_2} \right) \delta((p_1 + p_2)^2 - M^2) \times \frac{d^3p_1}{E_1} \frac{d^3p_2}{E_2} \frac{1}{\left( \frac{[E \frac{dR}{d^3p}] d^3p}{E} \right)}, \quad (7)$$

where the rate for singles production is parameterized according to the following [8]:

$$E_2 \frac{dR}{d^3p} = N e^{-E/T}, \quad (8)$$

with the normalization constant of  $N = 5 \times 10^{-3} \text{ fm}^{-4} \text{ GeV}^{-2}$ . Using this, a convenient expression for the rate of singles producing accidental doubles is

$$\frac{dR}{dM^2} = \frac{N\pi}{T} M \int_0^\infty dz \exp \left[ - (M/T) \left( z + \frac{1}{4z} \right) \right]. \quad (9)$$

The result for unrelated singles appearing as doubles is presented in Fig. 3. It can be rather simply understood since the rate for diphotons is of the order  $\alpha^2$  whereas the rate for unrelated singles contributing to a diphoton mass spectrum is of the order  $\alpha^2 \alpha_s^2$ . The extra factor of  $\alpha_s^2$  accounts for most of the difference between the quark–antiquark result as compared with the result from the singles.

#### 5 Form factors

Hadronic states treated within an effective field theory do not accurately reflect the fact that these are not point

particles. Indeed, the extended size of the hadrons can affect interactions, cross sections, and ultimately affect rates and yields. Consistently introducing higher-order contributions is somewhat nontrivial but is often effectively accomplished simply by imposing momentum-dependent form factors at each of the three-point vertices. Such form factors take into account off-shell effects due to non-point-like interactions. The specific form taken here is

$$f(t) = \frac{\Lambda^2 - m^2}{\Lambda^2 - t}, \quad (10)$$

where  $m$  is the mass of the off-shell meson and  $\Lambda$  is a parameter related to the spatial extent of the meson. The parameter  $\Lambda$  is taken to be 1 GeV, typical of hadronic energy scales.

Gauge invariance is immediately lost in such descriptions. However, it can be restored by modifying the contact (four-point) graph to reflect a general expansion over all possible Lorentz structures for the given incoming and outgoing four-momenta. The resulting full amplitude must consistently conserve currents for both of the final-state photons. These conditions specify the expansion coefficients needed in order to recover a completely gauge invariant amplitude. The method consistently incorporates proper four-momentum dependences for  $t$  and  $u$  channel graphs, and it allows general expressions to be taken for the form factors. Again, the monopole form in (10) is taken here.

The results for pion annihilation are reported in Fig. 4 with and without the form factor effects. As is typical of these types of studies, the further off-shell that the intermediate particles are pushed, the greater is the suppression due to the form factors. For a small invariant mass the off-shell region is only partially probed, and thus the form factor effects are small, while for high masses the off-shell region is more fully probed. Form factors are responsible for a suppression of roughly a factor of 2 for small masses and up to an order of magnitude for higher masses.

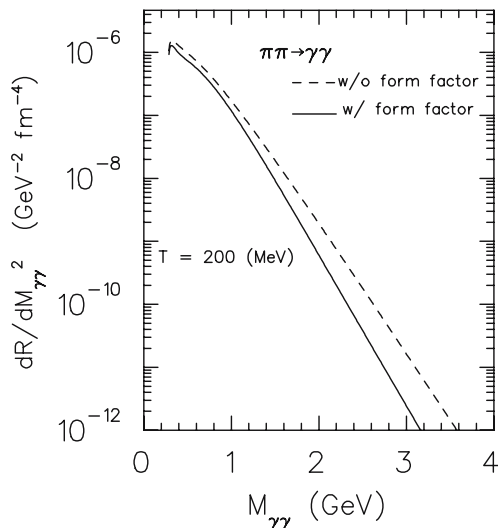


**Fig. 4.** Pion–pion annihilation rates with and without form factors introduced

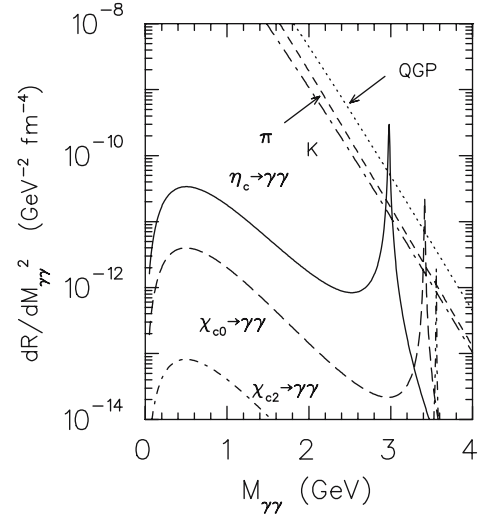


**Fig. 5.** Rate for producing photon pairs from leading charmonium states as compared with quark–antiquark (dotted) and hadron–hadron annihilation (dashed for pions, dot-long-dashed for kaons) at  $T = 200$  MeV

## 6 Charm sector

Charmonium can also decay into two-photon final states. The processes with the largest two-photon branching rates turn out to be  $\eta_c \rightarrow \gamma\gamma$ ,  $\chi_{c0} \rightarrow \gamma\gamma$ , and  $\chi_{c2} \rightarrow \gamma\gamma$ . The full widths for these particles suggests that thermal decay within the fireball is possible. Thus, it makes sense to compare the rate for charmonium states decaying to diphotons with the “background” of hadronic processes. If the charm states show structure in the invariant mass distribution, they could be excellent candidates for exploring charmonium suppression. In the absence of suppression, charmonium would be visible in the mass spectrum, whereas it would disappear if charmonium were dissolved in the early quark phase of the heavy-ion reaction.

In Fig. 5 the rates for charmonium decay into diphotons using the results from (6) are shown. Thermal charmonium decay into diphotons is comparable to quark–antiquark annihilation and hadron–hadron annihilation but is greater at the peaks and is therefore visible. The suggestion is therefore that it might be possible to use charmonium states for a QGP diagnostic since suppression of the  $\eta_c$  would signal quark–gluon degrees of freedom.

## 7 Summary and conclusions

Diphotons have been studied for their usefulness as a tool for robust thermometry and for spectroscopy. The rate for producing photon pairs from quark matter has been compared with the rate from hadronic matter. Processes within the hadronic matter included not only hadron–hadron annihilation but also resonance decays of various sorts. A rich spectrum of hadronic contributions seems possible as the thermal rate for decay to photon pairs shines above the

background. This immediately suggests the possibility of establishing a baseline rate and yield, but then searching for collective effects which could modify the spectral properties of the mesons [9].

Charmonium decay into diphotons is strong enough to be visible in the mass spectrum above the annihilation background. Suppression of the charmonium might possibly be visible by studying diphotons in the appropriate mass range to probe the charmonium states. Adding to the list of QGP diagnostics is clearly a desirable circumstance.

The outlook for further studies using diphotons is to more fully develop the hadron rates with form factor effects taken into account. Also, a model for the spacetime evolution of the system generated in heavy-ion reactions is needed in order to be able to predict diphoton yields. The results for the relative rates are strongly suggestive but it is important to draw conclusions based on final yields and only after appropriate experimental detector resolution is implemented.

*Acknowledgements.* This work was supported in part by the National Science Foundation under grant number PHY-0555521.

## References

1. T. Peitzmann, M. Thoma, *Phys. Rep.* **364**, 175 (2002)
2. C. Gale, K.L. Haglin, *Quark Gluon Plasma* (World Scientific, 2004) **3**, (2004) 364–429
3. See Proceedings of Quark Matter 2005, Budapest Hungary, 4–9 August, 2005
4. R. Rapp, J. Wambach, *Adv. Nucl. Phys.* **25**, 1 (2000)
5. E. Braaten, R.D. Pisarski, *Nucl. Phys. B* **337**, 569 (1990)
6. R. Baier, H. Nakkagawa, A. Niegawa, K. Redlich, *Phys. Rev. D* **45**, 4323 (1992)
7. K.L. Haglin, C. Gale, *Phys. Rev. C* **63**, 065 201 (2001)
8. J. Kapusta, P. Lichard, D. Seibert, *Phys. Rev. D* **44**, 2774 (1991)
9. K.L. Haglin, to be published